Article

Activation of sub 2 nm Water Soluble and Insoluble Standard Ions with Saturated Vapors of Butanol in a Boosted TSI ultrafine CPC

Michel Attoui [1],* and Juha Kangasluoma [2]

[1]   LISA, UMR7583, Institut Pierre Simon Laplace (IPSL), Université Paris-Est-Créteil, Université de Paris, 61 Avenue du Général de Gaulle, 94010 Créteil, France
[2]   Department of Physical Sciences, University of Helsinki, P.O. Box 64, 00014 Helsinki, Finland; juha.kangasluoma@helsinki.fi
*   Correspondence: attoui@u-pec.fr

check for updates

Abstract: Tetraheptylammonium bromide (THABr), tetrabutylammonium bromide (TBABr) and tetraethylammonium bromide (TEABr) dissolved in methanol or water methanol mixtures (~1 mM) produce via positive electrospray atomization and high resolution classification electrical classification standard clean ions (monomer and dier) which are singly charged. THABr is hydrophobic and insoluble in water, TBABr and TEABr are hygroscopic and water soluble (0.6 and 2.8 kg/L respectively). These ions are used to study the effect of hygroscopicity on the activation of aerosol particles in the sub 2 nm range via the detection efficiency measurement of a boosted ultrafine TSI condensation particle counter (3025A). Water solubility of particles seems to play a role in the activation and growth with butanol vapor in the CPC (condensation particle counter) independently of the size.

Keywords: CPC; DMA; water soluble; sub 2 nm particles; nucleation; activation; growth; butanol

1. Introduction

The first commercial continuous sequential flow butanol condensation particle counter (model 3020 butanol CPC or CNC (condensation particle counter or condensation nucleus counter) based on the work of Bricard and coworkers in France and Sinclair and coworkers in US) introduced by TSI (TSI Inc., St. Paul, MN, USA) was capable of counting single particles with diameters (Dp) larger than 10 nm with 50% detection efficiency [1]. The CPC was calibrated against an aerosol electrometer (AEM) with sodium chloride particles produced with a pneumatic atomizer and size classified with cylindrical Hewitt DMA commercialized by TSI [2,3]. Madelaine and Metayer [4] (1980) discovered that the detection efficiency of that CPC depends of the chemical composition of the particles used for the calibration. They showed that hydrophilic and water soluble particles (H_2SO_4; NaCl) are detected with higher efficiency than hydrophobic or insoluble particles (V_2O_5) of the same size and same electrical charge [5].

The ability of the CPCs to detect very low particle concentrations and electrically neutral particles are their main advantage compared to the aerosol electrometers. The downside and limiting factor is the size dependent detection efficiency, defined as the ratio of the particle number concentration measured by a CPC and the concentration of a reference instrument given by an aerosol electrometer, which limits the usability of CPCs in the sub-3 nm size range.

J.C. Wilson and coworkers [6,7] described and built an instrument (based on the TSI 3020 model) to operate in aircrafts to study stratospheric aerosols (40–400 mbar). The design priorities of the instrument included fast response time and the ability to count accurately concentrations of ultrafine particle at low pressures. To reduce the response time of the instrument and diffusion losses, filtered

sheath air flow confines aerosol flow to the center streamline of the condenser of the CPC. With this design all the sampled particles are exposed to similar supersaturation profiles in the condenser. This instrument and its successors have played an important role in NASA's research on stratospheric (8–21.5 km) ozone depletion [8].

Stolzenburg and McMurry [9] used Wilson's design to extend the minimum detectable particle size of a CPC from 10 to 3 nm with 50% detection efficiency at one bar (atmospheric pressure). The particles are exposed to the maximum supersaturation in the centerline of the condenser with the help of the sheathed clean air which minimizes the diffusion losses in the other hand. However, the detection efficiency drops rapidly to zero for particles smaller than 3 nm. This prototype was used by TSI to introduce their commercial version model 3025 (ultrafine CPC). Kesten et al. [10] used singly charged size selected sodium chloride and silver particles for the calibration of the 3025 down to 2 nm.

Sodium chloride particles and non-soluble particles of DOP (dioctyl phthalate) were used in 1979 during a workshop in Vienna University [11] to study the effect of solubility and wettability on the Kelvin diameter measurement of large particles (Dp > 13 nm) with the 'size-analyzing nuclei counter' (SANC). The particles were produced by atomization and classification [12]. The conclusion of these studies show that the detection efficiency (DE) is higher for water soluble particles for the same diameter than the non-water soluble particles.

Scheibel and Porstendörfer [13,14] in a theoretical and experimental studies used insoluble (hydrophobic) particles of silver and hydrophilic particles of NaCl to measure the detection efficiency of the General Electric water expansion CPC down to 2 nm. The particles were produced by evaporation-condensation material in the well-known Scheibel and Porstendörfer generator [15]. Since that time the experimental studies on heterogeneous nucleation, ion induced nucleation and 'calibration' of condensation particles counters have been done with hydrophilic particles of sodium chloride and hydrophobic silver particles. Recently aerosol particles larger than 2 nm of sucrose generated via electrospray with electrical charge reduction are used for hydrophilic and water soluble particles [16]. On the other hand evaporation-condensation with glowing resistively heated wire generator [17] is used intensively for the generation of hydrophobic insoluble particles [18–21].

Laboratory generation of sub 2 nm particles and size classification with high resolution diameter are accessible with the help of cost effective electrospray sources followed by high resolution and high flow DMAs thanks to the work of Prof. Juan Fernandez de la Mora and coworkers at Yale University [22–24]. Sub 2 nm standard ions (in terms of mass and mobility) are produced with this method with relatively high concentrations (up to 10^6 pcm^{-3}) and few liters per minute flowrate (up to 15 lpm) with a minimum diameter resolution of 40 [25].

CPCs detectors particles smaller than 3 nm are needed (in the atmosphere, industrial process, combustion, etc.) to measure nucleation rates, understand nucleation and ion induced nucleation. Ultrafine butanol based CPCs have shown their ability to detect sub 3 nm particles at high supersaturations close to the homogeneous nucleation [18,26] or with low level of homogeneous nucleation [27]. The studies have used standard hydrophobic ions (tetra methyl ammonium bromide, tetraheptylammonium bromide, and tetra dodecyl ammonium bromide) in positive mode mostly [28,29].

The condensation particles counters are characterized by their cut off. The cut off or D_{50} is the smallest particle diameter detected by the counter with a detection efficiency of 50%. The particle diameter at which the counter sees no particles is called D_0 or LSDL for lower size detection limit. Recently the generation of water soluble standard singly charged positive ions in the sub 2 nm size range has been demonstrated [30]. These ions are used in this paper for the first time to measure the lower size detection limit (LSDL) with a boosted butanol based 3025 TSI model.

The LSDL or activation diameter D_0 depends on different variables. Some of them are macroscopic, with a role defined to first approximation by classical homogeneous or ion-induced nucleation theory. The most important parameter for neutral particle activation is a characteristic length L defined by the surface tension γ of the working fluid and the thermal energy [31] kT, L = $(kT/\gamma)^{1/2}$. Charged

particles are more easily activated than neutral particles, to the point that even sub-nanometer ions can be grown into drops in a diversity of vapors, including not only water [32] (Wilson, 1897), but other organic substances such as dioctylphtalate [33], ethylene glycol [34] and diethylene glycol [35–37].

The LSDL is influenced by the chemical composition of the particles, the wettability of the particle surface by the condensing vapor, the charge state of the particles and the particle solubility in the working fluid vapor. Theoretical and experimental recent works show that these effects are stronger when the sizes of sampled particles are smaller and smaller [38,39].

The ability of butanol to activate particles in the sub 2 nm has been already demonstrated recently [40,41]. Maisser and Hogan [42] used a high transmission and high resolution differential mobility coupled to a mass spectrometer to study the activation of metal alkyl with butanol and nonane vapors. Attoui [28] used a commercial condensation particle (TSI 3776 Model) to study the detection efficiency of the boosted instrument. Size analyzing nucleus counter (SANC) and a commercial ultrafine CPC (TSI 3776) were used at the University of Vienna [41] to study the heterogeneous nucleation of water soluble (Sodium Chloride) and water non soluble silver particles larger than 2.5 nm.

The goal of the present study is a first attempt to quantify the effect of the hygroscopicity and or water solubility on the activation of sub 2 nm positive singly charged ions with butanol vapor with a boosted commercial CPC. The study uses the TSI 3025 ultrafine CPC for which the difference of temperatures between the saturator (Ts) and condenser Tc (ΔT) of 38 °C can reach with concentration of homogeneous particles (background) less than 10 pcm^{-3}.

2. Experimental Section

The experimental set-up given in the Figure 1 is mainly based on a high resolution sub 2 nm particle generator and a boosted ultrafine condensation particle counter (based on a TSI CPC 3025) with variable supersaturation as a detector. The experimental setup is the classical setup and method used during the last few decades for the generation of sub-10 nm and detection-efficiency measurements with a high particle size resolution. It is widely documented in the literature [25,42–47].
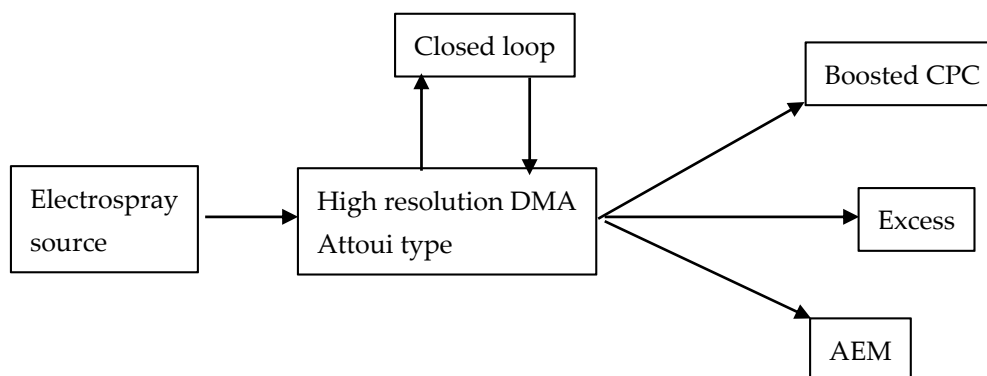
Figure 1. Experimental set up used in this study.

As stated above, the first part of this study is dedicated to the quantification of the effect of the temperature difference between the saturator and the condenser on the activation of the three different standard ions by saturated butanol vapor inside a boosted ultrafine CPC. In this study the temperature of the condenser Tc is kept constant and equal to 8 °C (the manufacturer TSI uses 10 °C in the standard conditions). The maximum temperature of the saturator is limited to 44 °C to avoid homogeneous nucleation. The background is limited to a maximum of 10 particles per cubic centimeter (pcm^{-3}). The maximum concentration at the outlet of the DMA is limited to 10^5 pcm^{-3} to prevent high coincidence errors in the CPC and agglomeration in the whole system (generation-detection line). The limitations of the concentration to 10^5 pcm^{-3} is archived by increasing the distance of the electrospray source to

the inlet of the DMA. Indeed the diffusion losses of the sub 2 nm are l dependent of the length of the transport line.

A flowrate of 8 L per minute (lpm) of compressed and filtered air is pushed in the electrospray source connected to the DMA. The aerosol electrometer (AEM), constituted by a Filter Faraday Cage (electrical charge collector) and a Keithley electrometer (model 6517), samples 5 lpm. The CPC samples 1.5 lpm and the excess flow is kept at 1.5 lpm during the experiments. A computer program ramps the high voltage applied to the inner electrode of the DMA. The signal of the electrometer and the CPC are recorded as a function of the applied voltage. The ion mobility calibration of the sheath flowrate of the DMA at fixed experimental conditions, tetraheptylammonium bromide monomer $(C_7H_{15})4N^+$ with the reference mobility value of Z = 0.962 cm2/Vs was used [22].

The high resolution generator is a combination of a home-made electrospray source [22] and a high resolution Attoui-type DMA [44]. Salt solutions at typically ~10 mM concentrations in methanol, or ethanol, or acetonitrile or water methanol mixture are electrosprayed from a sharpened tip of either 20 or 40 μm ID silica capillaries. The liquid flow rate in the capillary is close to the minimal value at which a steady Taylor cone-jet could be stabilized. The DMA has been widely described in the literature [44,45]. Here only a brief description is given.

DMAs operate with two flows: Qa, the aerosol (or sample) flow and Qs, a filtered, aerosol-free sheath flow. The size resolution of a DMA is given by the ratio Qa/Qs. Typical DMAs are used with Q_a = 1 to 4 and Qs = 5 to 20 L per minute (lpm). The Attoui DMA [45] used in this study was operating at Qa = 10 and Q_s = 300 lpm. The resolution of such DMA exceeds 25. High Qa/Qs ratio is the key parameter for selecting aerosol particles with high resolution. A high-resolution DMA is needed because the particles used in this study to measure the detection efficiency are in a very narrow size range (between 1 and 2 nm). The flow control in the closed loop of the DMA uses a high-flow TSI flowmeter to control the flow rate. Tetraheptylammonium bromide is used as a standard to calibrate the flow rate of the DMA at the beginning of the experiments and to check the stability of the system afterwards. Then different type of aerosol can be injected into the DM to extract the desired ions and or size. The calibration factor k, determined by calibration with the monomer of the tetraheptylammonium bromide (ΔTHA^+), is needed to relate the particle mobility Z to the measured voltage V of the DMA called V_{dma} in volts. The factor k is then given by the following expression:

$$k = ZV/Q = cst,$$

where k is constant if Q is constant. Q is the total flow rate in the DMA, which in our case can be approximated to the sheath flow rate. Q is assumed to be constant hereafter. Z is the mobility diameter and V the voltage in the DMA. The mobility diameter Zs of the monomer THA$^+$ is selected by the DMA for a voltage Vs. Zs = (1/1.03) cm^2/VS is given by the literature [22].

The flowrate in the condenser and in the capillary of the CPC are kept constant (0.3 and 0.03 lpm). The size dependence of the detection efficiency (DE) of the instrument is used in this study measure the effect of the solubility in water of sub 2 nm positively charged particles on their activation by butanol vapor.

Ude and Fernandez de la Mora [22] have introduced the concept and method of producing mobility selected clean molecules with electrospray method (in positive mode). They use a high resolving power DMA working with high sheath flowrate with large tetra-alkyl ammonium halide salts (bromide or iodide) dissolved in HPLC grade alcohol (methanol or ethanol) In positive mode hydrophobic and water insoluble tetraheptylammonium bromide (THABr) exhibits two well resolved very sharp singly charged peaks. Figure 2 shows size distribution (mobility diameter in nm) spectra of tetrabutylammonium bromide (TBABr) (A) and tetraethylammonium bromide (TBABr) (B) with an aerosol electrometer as a detector of the DMA. Both compounds produce two sharp and well defined peaks identified as the monomer and dimer of the corresponding salt.
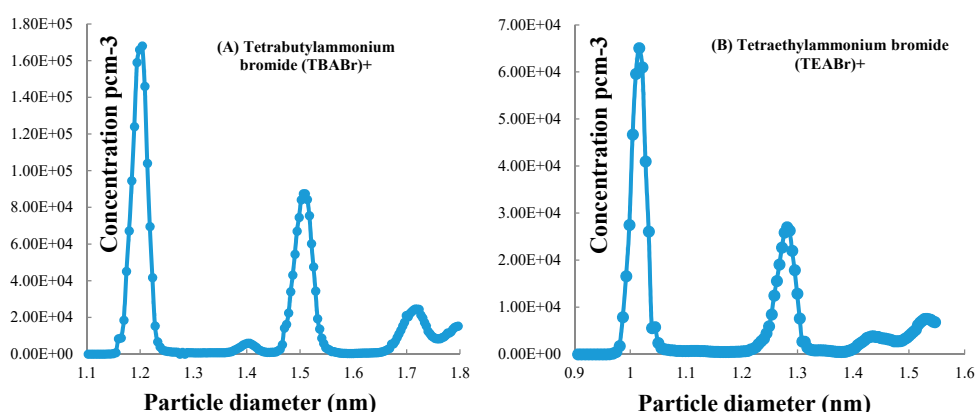
Figure 2. Mobility size distribution of positively electrosprayed cluster ions the tetraheptylammonium bromide (TBABr) and tetrabutylammonium bromide (TBABr) with an aerosol electrometer.

It is also the case of the third compound, tetraheptylammonium bromide, (THABr) used in this study. The two peaks corresponding to the monomer and the dimer are used in this study. The results are compared to the DE measurement in the same conditions of two hydrophilic and water soluble ions: TBABr and TEABr.

The Table 1 gives the characteristics of these three ions. TEABr is highly soluble with the lowest molecular weight. The mobility diameters of the produced ions are proportional to the molecular weight. THABr$^+$, TBABr$^+$, TEABr$^+$ are with a plus sign because they are sprayed in positive mode.

Table 1. Characteristics of the standard ions (dissolved in water methanol) used in the study.

| Compound	Molecular Weight	Solubility in H$_2$O	Hydrophilic	Hydrophobic
THABr	490.6 g/mol	No	No	Yes
TBABr	322.37 g/mol	0.6 kg/liter	Yes	No
TEABr	210.15 g/mol	2.8 kg/liter	Yes	No

3. Results

The ability of the laminar ultrafine TSI CPC 3025A to activate sub 2 nm particles with butanol as working fluid by increasing the temperature difference between the saturator and the condenser has been recently demonstrated [18]. These results have been confirmed with different chemical composition of sub 2 nm standard and non-standard hydrophobic and non-water soluble particles [26]. The effect of the solubility of particles in water on the particle growth or CPC detection efficiency is now possible since the production of standard particles with electrospray of water soluble compounds have been discovered [30].

The goal of the study is not a high accuracy measurement of the detection efficiency of the instrument. The main goal is to measure the effect of water solubility of particles on their activation or not by butanol. Our results show a higher activation of water soluble particles than the activation of non-water soluble sub 2 nm standard particles. The first step in the study is to find the conditions in terms of ΔT to activate the monomer of the THABr widely used as standard ion for calibration of CPCs. The positively charged monomer of THABr ([CH$_3$(CH$_2$)$_4$N$^+$ or THA$^+$) exhibits a mobility diameter of 1.47 nm. The dimer [CH$_3$(CH$_2$)$_6$]$_8$N$_2$Br$^+$ or [Br$^-$(THA$^+$)$_2$] has a mobility diameter of 1.78 nm [22]. The THABr ions are known to be hard to activate.

Figure 3 gives the mobility diameter distributions of the THABr as a function of the voltage of the DMA. The monomer emerges at 362 volts, the dimer at 534 Volts. The results in the Figure 3A (on the left) are given by the DMA when an aerosol electrometer is used as a detector of the DMA. The results in the Figure 3B (on the right) are given by the DMA when a boosted butanol CPC with different ΔTs as a detector. In this study the temperature of the condenser is kept constant at 8 °C.

8 °C rather than 10 °C is chosen to have 'large' ΔTs with 'low' saturator temperatures. High saturator temperatures may cause neutral and or ion evaporation from the clusters during their time of flight in the saturator [48,49].

The monomer and dimer of the THABr are separated by another small peak (at 418 Volts) more 'visible' in the Figure 3B in which the CPC is used as detector thanks to its sensitivity. This peak appears when the DMA is working in closed loop without dryer to remove volatile solvent (methanol, ethanol or acetonitrile) vapors introduced in the sheath gas by the droplets produced in the electrospray source [24,49,50]. That small peak is produced by the solvated monomer of the THABr with these vapors and eventually water vapor in case the carrier gas used through the electrospray source is not dry N_2 or air from a cylinder. In our case the carrier gas used in the electrospray chamber is a 'dry' compressed and filtered laboratory air. The apparently continuous background rising approximately at the position of the trimer is associated with multiply charged ions too numerous to produce distinct mobility peaks.
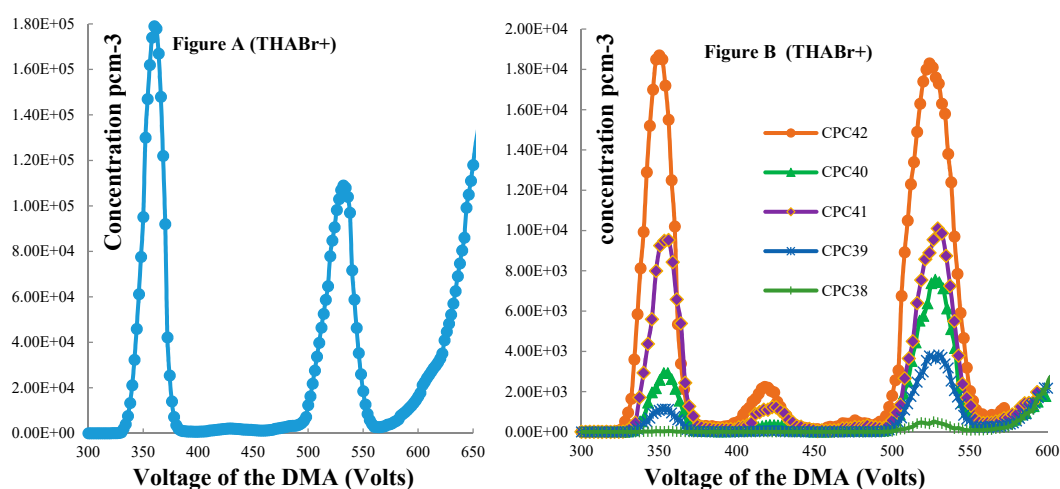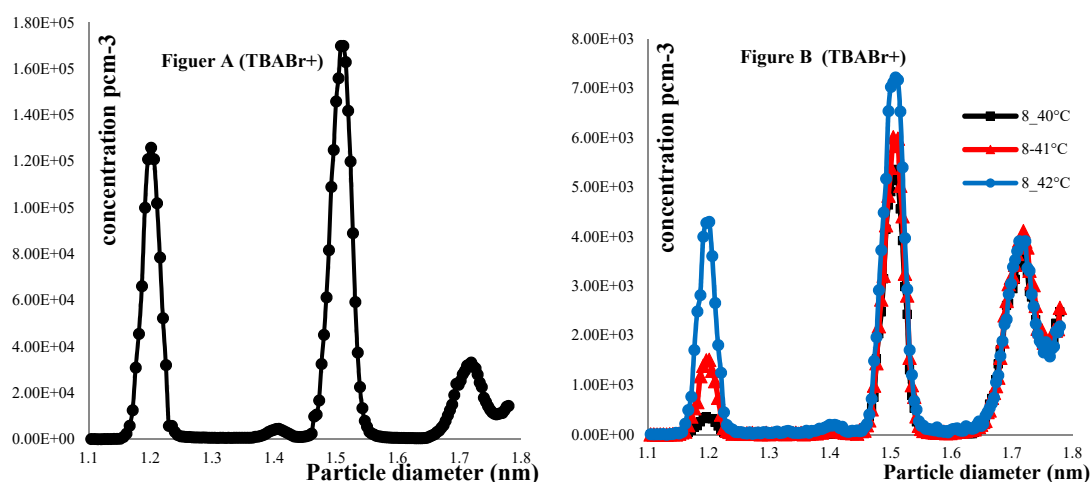

Figure 3. Mobility diameter distribution measurements of the tetraheptylammonium bromide as a function of the voltage of the DMA. Aerosol electrometer (AEM) was in use in the results given in the Figure (**A**) (left panel). Variable saturator temperatures CPC was in use for the results given in the Figure (**B**) (right).

The CPC starts to detect the THABr dimer (1.78 nm) when the temperature of the saturator is 38 °C (ΔT = 30 °C), but not the monomer. The monomer starts to emerge in the scans of the voltages of the DMA at only 39 °C (ΔT = 31 °C). As seen in the Figure 3B, 42 °C in the saturator and 8 °C in the condenser (ΔT = 36 °C) give enough (or measurable) signal for the monomer of the THABr and dimer.

TBABr, a quaternary ammonium salt with a bromide counter ion ($C_{16}H_{36}N^+Br^-$) is the second compound used in this study. With a lighter molecular weight (322.367 g/mol) compared to the THABr (490.71 g/mol) the monomer and the dimer exhibit lower mobility diameters, well defined peaks given in the Figure 4A,B.

Figure 4. Mobility measurements of the tetraheptylammonium bromide with a DMA. Aerosol electrometer was in use in the results given in the Figure (**A**) (left panel). Variable T CPC (condenser–saturator) was in use for the results given in the Figure (**B**) (right panel).

The mobility diameter of the monomer of the TBABr is 1.20 nm and the dimer is 1.51 nm which is very close to the monomer of the THABr (1.47 nm). With a difference of only 0.03 nm the mobility diameter can be assumed to be the same. In Figure 4A appears a peak with low signal at 1.40 nm. This peak cannot be associated to solvated monomer with volatile vapors present in the loop of the DMA as in the case of the THABr because of its low mobility. Indeed the diameter of the peak is close to the diameter of the dimer for solvation phenomena. It can be associated to contamination or impurities in the solvent (water/methanol in this case) or metastable multi charged ion.

The third peak at 1.72 nm is a mixture of the trimer of the TBABr and essentially multiply charged big clusters as already seen with the THABr trimer. This peak is not clean enough to be used as a standard. Therefore it cannot be used in the detection efficiency measurement. It cannot be used in nucleation studies either because multiply charged clusters tend to activate nucleation at considerably smaller size than singly charged ions. A slight level of contamination can greatly distort the picture in the case of the nucleation studies.

The Figure 4B gives the mobility diameter distribution of the TBABr monomer and dimer with a variable saturation CPC as a detector. The monomer is detected at a saturator temperature of 40 °C ($\Delta T = 32$ °C) with low level of signal (500 pcm^{-3}). At 42 °C in the saturator the signal is much higher (4.3×10^3 pcm^{-3}) with no homogeneously nucleated background.

TEABr, the third compound used in this study has the highest solubility in water (2.8 kg/L H_2O). Dissolved in a mixture of water-methanol (50/50 in volume) it gives via positive electrospray atomization and mobility selection 2 well defined sharp peaks. The peaks correspond to the monomer and dimer standard molecules with 1.01 nm and 1.28 nm mobility diameter respectively. The dimer of the TEABr (1.28 nm) exhibits a mobility diameter close to the monomer of the TBABr (1.20 nm).

Figure 5A gives the mobility diameter distribution of TEABr measured with the DMA and an aerosol electrometer as detector. The particle concentration measured with the electrometer is high especially for the monomer ($\sim 7 \times 10^4$ pcm^{-3}) and 2.5×10^4 particles per cubic centimeter of air for the dimer because the solution is diluted (~ 100 μM). The concentrations measured with a CPC as a detector of the DMA is lower but still high enough for $\Delta T = 38$ °C (8 and 42 °C) for example.
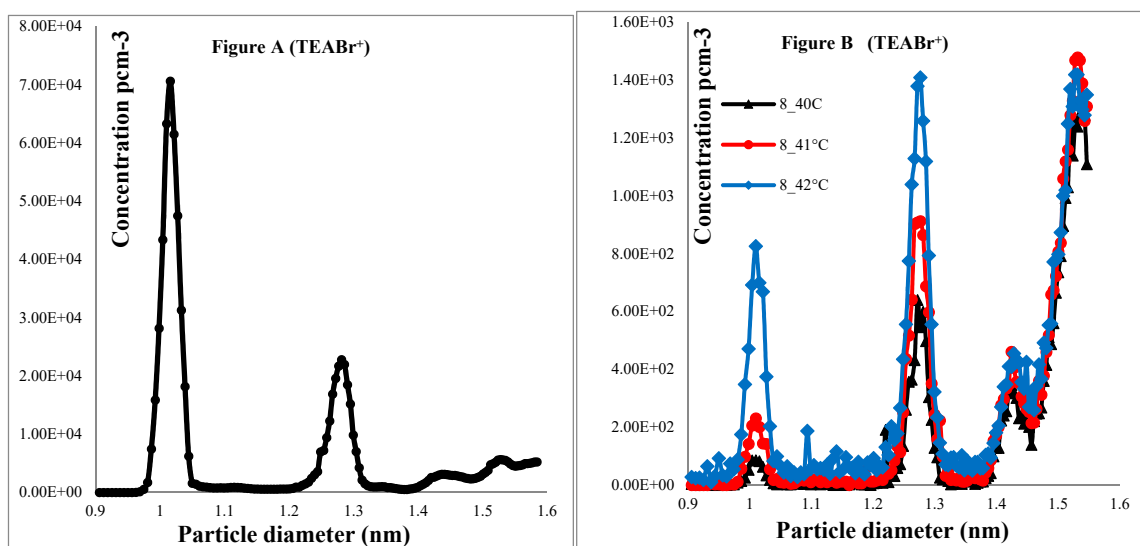
Figure 5. Mobility measurements of the tetraethylammonium bromide (TBABr) with a DMA. Aerosol electrometer was in use in the results given in the Figure (**A**) (left panel). Variable T CPC was in use for the results given in the Figure (**B**) (right panel).

The detection efficiency is measured for each peak (monomer and dimer) at constant voltage during 2 min (120 values) with the aerosol electrometer as a reference and the CPC in parallel. A median detection efficiency is then calculated as the ratio of the concentrations detected by a CPC and the aerosol electrometer. The calculations are made without any correction. The results presented in the Figure 6 are raw detection efficiencies.
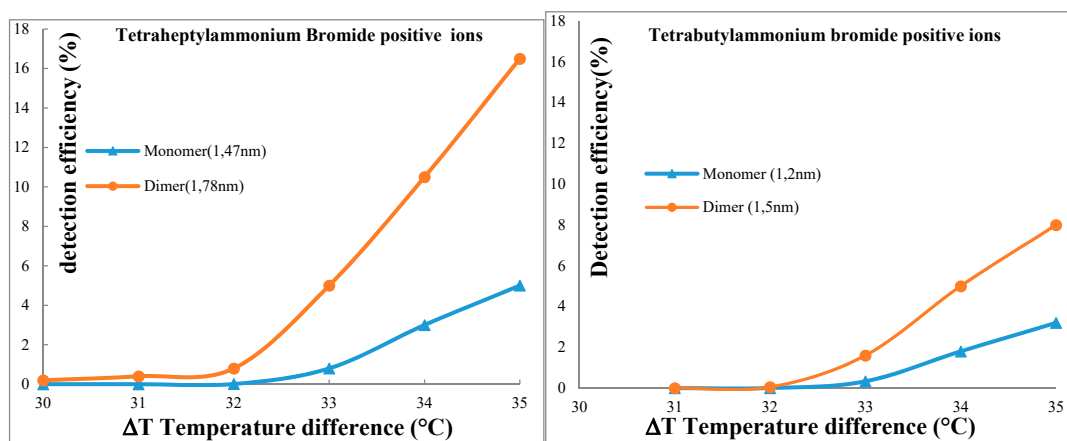
Figure 6. Detection efficiency of the CPC for THABr and TBABr ions for different Ts.

The Figure 6 shows the measured detection efficiency of the CPC with hydrophobic THABr and hydrophilic TBAB. The dimer of the TBABr and the monomer of the THABr are close in terms of diameter (1.5 and 1.47 nm). The detection efficiency is however higher for the hydrophilic ion than for the hydrophobic one.

Figure 7 gives the measured detection efficiency of the CPC for positive ions (monomer and dimer) of TEABr. This salt is highly soluble in water than the first ones (THABr and TBABr). This salt gives the smallest monomer (1.01 nm) and the smallest dimer (1.28 nm) but the detection efficiency is high and comparable to the detection efficiency for the THABr ions which are bigger in terms of masses and mobility diameters.
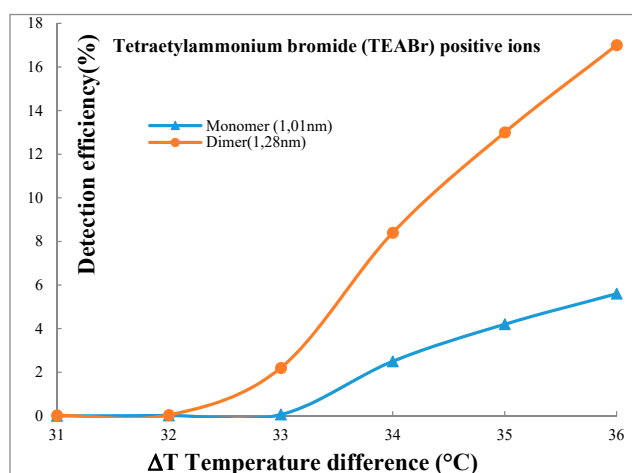
Figure 7. Detection efficiency of the CPC for TEABr and TBABr ions for different Ts.

4. Discussion and Conclusion

Electrospray atomization used with a high resolution differential mobility analyzer provides access to the generation of singly charged sub 2 nm size range particles with molecules of dissolved compounds (mostly tetra alkyl ammonium halides) in alcohol or water/alcohol mixtures. These molecules are used as molecular standards in aerosol science and mass spectrometry field since their introduction [22,33]. They offer the possibility of studying the effect of their water solubility property on the nucleation, detection efficiency of instruments like CPCs measurements, deliquescence etc.

THABr, TBABr, and TEABr molecules (positively charged monomers and dimers) are used in this study for the first time with a commercial version of CPC (TSI 3025 ultrafine CPC). The CPC is boosted by increasing the temperature difference between the saturator and the condenser. Monomer and dimer of each salt give six different mobility diameters ranging from 1.01 nm to 1.78 nm corresponding to a mass range from 209 amu to 900 amu.

Only the THABr is hydrophobic and water insoluble salt. THABr, TBABr and TEABr are butanol soluble. The THABr is the most soluble in butanol. The solubility has been noticed by eye in the laboratory. A small amount of each salt (~1 mg) is dropped inside a vial containing 0.5 mL of butanol. THABr is dissolved more or less instantaneously. TBABr and TEABr are dissolved only after shaking by hand the small vial. It was impossible to find the solubility values of these salts in butanol in the literature.

The first part of the study focuses on the characterization of the ultrafine condensation particle counter (TSI model 3025A) in the sub 2 nm rage in terms of detection by increasing the temperature difference between its saturator and condenser. As seen in the Figure 2, particles of THABr are activated in the CPC at a temperature difference of 32 °C. A temperature of 8 °C in the condenser rather than 10 °C in previous studies [18,25,28] allows large ΔTs with low temperatures in the saturator.

With ΔT = 36 °C the CPC gives detectable signal even for the smallest ion used in the study (monomer of TEABr) with very small homogeneous nucleation signal (less than 10 pcm^{-3}). There is no ion activation in the CPC for ΔT smaller than 31 °C (8 °C and 39 °C). The CPC shows that particles as small as 1 nm mobility diameter (0.7 nm mass diameter) can be activated in a laminar flow CPC with butanol as working fluid. The low activation efficiency can be explained by the sampling losses in the CPC because of the low aerosol flowrates (0.3 lpm in the condenser and 0.03 lpm in the capillary) and by the properties of the butanol as a working fluid [31,35]

The detection efficiency of the smallest ion (monomer of the TEABr 1.01 nm) reaches 4.2% at a ΔT = 35 °C. The dimer (1.28 nm) is seen by the CPC with a DE of 13%. A difference of 10 % appears with the DE for the monomer of the TBABr with 1.20 nm diameter. There is a difference of 0.08 nm between the ions but it's hard to think that this difference is introduced by the size and not by the higher solubility in water of the TEABr.

Although the three ions are soluble in butanol, the fact that the tetra ethyl ammonium ion is activated with higher detection efficiency whilst being the most mobile (1.01 nm) than the lightest ion, would suggest that the solubility in water of the particles or ions play a major role for understood reasons. Care must be taken in the other hand about the hypothesis of water soluble and or insoluble in water of sub 2 nm particles produced by water soluble and or insoluble powders. A water CPC sensitive to particles of sub 2 nm with high enough detection efficiency could be used to confirm these primary results.

References

1. Agarwal, J.K.; Sem, G.J. Continuous flow, single particle-counting condensation nucleus counter. *J. Aerosol Sci.* **1980**, *11*, 343–357. [CrossRef]
2. Hewitt, G. The charging of small particles for electrostatic precipitation. *AIEE Trans.* **1957**, *76*, 300–307. [CrossRef]
3. Knutson, E.O.; Whitby, K.T. Aerosol classification by electric mobility: apparatus, theory, and applications. *J. Aerosol Sci.* **1975**, *6*, 443–451. [CrossRef]
4. Madelaine, G.; Meteyer, Y. Note. *J. Aerosol Sci.* **1979**, *11*, 358. [CrossRef]
5. Kangasluoma, J.; Attoui, M. Review of sub-3 nm condensation particle counters, calibrations and cluster generation methods. *Aerosol Sci. Technol.* **2019**. [CrossRef]
6. Wilson, J.C.; Blackshear, E.D.; Hyun, J.H. An Improved Continuous-Flow Condensation Nucleus Counter for Use in the Stratosphere. *J. Aerosol Sci.* **1983**, *14*, 387–391. [CrossRef]
7. Wilson, J.C.; Blackshear, E.D.; Hyun, J.H. The function and response of an improved stratospheric condensation nucleus counter. *J. Geophys. Resh.* **1983**, *88*, 6781–6785. [CrossRef]
8. Wilson, J.C.; Loewemstein, M.; Fahey, K.W.; Gary, G.V.; Chan, K.R. Observations of Condensation Nuclei in the Airborne Antarctic Ozone Experiment Implications for New Particle Formation and Polar Stratospheric Cloud Formation. *J. Geophys. Res.* **1989**, *94*, 16437–16448. [CrossRef]
9. Stolzenburg, M.R.; McMurry, P.H. An Ultrafine Aerosol Condensation Nucleus Counter. *Aerosol Sci. Technol.* **1991**, *14*, 48–65. [CrossRef]
10. Kesten, J.; Reineking, A. Porstendorfer Calibration of a TSI 3025 Condensation Particle Counter. *Aerosol Sci. Technol.* **1991**, *15*, 107–111. [CrossRef]
11. Liu, B.Y.H.; Pui, D.Y.H.; McKenzie, R.L.; Agarwal, J.K.; Jaenicke, R.; Pohl, F.G.; Reischl, G.; Preining, O.; Szymanski, W.; Wagner, P.E. Measurements of Kelvin-Equivalent Size Distributions of Well-Defined Aerosols with Particle Diameters > 13 nm. *Aerosol Sci. Technol.* **1984**, *3*, 107–115. [CrossRef]
12. Liu, B.Y.H.; Pui, D.Y.H. A Submicron Aerosol Standard and the Primary, Absolute Calibration of the Condensation Nuclei Counter. *J. Colloid Interface Sci.* **1974**, *47*, 155–171. [CrossRef]
13. Scheibel, H.G.; Porstendorfer, J. Counting Efficiency and DetectionLimit of Condensation Nuclei Counters for Submicrometer Aerosols.1. Theoretical Evaluation of the Influence of Heterogeneous Nucleationand Wall Losses. *J. Colloid. Interf. Sci.* **1986**, *109*, 261–274. [CrossRef]
14. Scheibel, H.G.; Porstendörfer, J. Counting efficiency and detection limit of condensation nuclei Counters for submicrometer aerosols II. Measurements with Monodisperse Hydrophobic Ag and HygroscopicNaCI Aerosols with Particle Diameters between 2 and 100 nm. *J. Colloid. Interf. Sci.* **1986**, *109*, 275–291. [CrossRef]
15. Scheibel, H.G.; Porstendörfer, J. Generation of monodisperse Ag- and NaCl-aerosols with particle diameters between 2 and 300 nm. *J. Aerosol Sci.* **1983**, *14*, 113–126. [CrossRef]
16. Kupc, A.; Bischof, O.; Tritscher, T.; Beeston, M.; Krinke, T.; Wagner, P.E. Laboratory characterization of a new nano-waterbasedCPC 3788 and performance comparison to an ultrafinebutanol-based CPC 3776. *Aerosol Sci. Technol.* **2013**, *47*, 183–191.
17. Peineke, C.; Attoui, M.B.; Schmidt-Ott, A. Using a Glowing WireGenerator for Production of Charged, Uniformly Sized Nanoparticles atHigh Concentrations. *J. Aerosol Sci.* **2006**, *37*, 1651–1661. [CrossRef]

18. Kuang, C.A.; Chen, M.D.; McMurry, P.H.; Wang, J. Modification of Laminar Flow Ultrafine Condensation Particle Counters for the Enhanced Detection of 1 nm Condensation Nuclei. *Aerosol Sci. Technol.* **2012**, *46*, 309–315. [CrossRef]

19. Kangasluoma, J.; Junninen, H.; Lehtipalo, K.; Mikkila, J.; Vanhanen, J.; Attoui, M.; Sipila, M.; Worsnop, D.; Kulmala, M.; Petaja, T. Remarks on Ion Generation for CPC Detection Efficiency Studies in Sub-3-nm Size Range. *Aerosol Sci. Technol.* **2013**, *47*, 556–563. [CrossRef]

20. Kangasluoma, J.; Ahonen, L.; Attoui, M.; Vuollekoski, H.; Kulmala, M.; Petaja, T. Sub 3 nm particle detection with commercial TSI 3772 and Airmodus A20 Fine condensation particle counters. *Aerosol Sci. Technol.* **2015**, *49*, 674–681. [CrossRef]

21. Kangasluoma, J.; Attoui, M.; Junninen, H.; Lehtipalo, K.; Samodurov, A.; Korhonen, F.; Sarnela, N.; Schmidt-Ott, A.; Worsnop, D.; Kulmala, M.; et al. Sizing of Neutral Sub 3 nm Tungsten Oxide Clusters using Airmodus Particle Size Magnifier. *J. Aerosol Sci.* **2015**, *87*, 53–62. [CrossRef]

22. Ude, S.; De la Mora, J.F. Molecular Monodisperse Mobility andMass Standards from Electrosprays of Tetra-Alkyl Ammonium Halides. *J. Aerosol Sci.* **2005**, *36*, 1224–1237. [CrossRef]

23. Fernandez de la Mora, J.; Kozlowski, K. Hand-Held DifferentialMobility Analyzers of High Resolution for 1-30 nm Particles: Design andFabrication Considerations. *J. Aerosol Sci.* **2013**, *57*, 45–53. [CrossRef]

24. Attoui, M.; Paragano, M.; Cuevas, J.; Fernandez de la Mora, J. Tandem DMA Generation of Strictly Monomobile 1–3.5 nm Particle Standards. *Aerosol Sci. Technol.* **2014**, *47*, 499–511. [CrossRef]

25. Kangasluoma, J.; Attoui, M.; Korhonen, F.; Ahonen, L.; Siivola, E.; Petaja, T. Characterization of a Hermann type high resolution differential mobility analyzer. *Aerosol Sci. Technol.* **2016**, *50*, 22–229. [CrossRef]

26. Kangasluoma, J.; Samodurov', A.; Attoui, M.; Franchin, A.; Junninen, H.; Korhonen, F.; Kurten, T.; Vehkamati, H.; Sipila, M.; Lehtipalo, K.; et al. Heterogeneous nucleation onto ions and neutralized ions. *J. Phys. Chem. C.* **2016**, *120*, 7444–7450. [CrossRef]

27. Sipilä, M.; Lehtipalo, K.; Attoui, M.; Neitola, K.; Petäjä, T.; Aalto, P.P.; O'Dowd, C.D.; Kulmala, M. Laboratory Verification of PHCPC'sAbility to Monitor Atmospheric Sub-3 nm Clusters. *Aerosol Sci.Technol.* **2009**, *43*, 126–135. [CrossRef]

28. Attoui, M. Activation of sub 2 nm singly charged particles with butanol vapors in a boosted 3776 TSI CPC. *J. Aerosol Sci.* **2018**, *126*, 47–57. [CrossRef]

29. Barmpounis, K.; Ranjithkumar, A.; Schmidt-Ott, A.; Attoui, M.; Biskos, G. Enhancing the detection efficiency of condensation particle counter for sub 2 nm particles. *J. Aerosol Sci.* **2018**, 44–53. [CrossRef]

30. Attoui, M. Generation of Water Soluble Standards Ions in the in the sub 2 nm range. In Proceedings of the Aerosol Technology Conference, Tampere, Finland, 15–17 June 2015.

31. Magnusson, L.E.; Koropchak, J.A.; Anisimov, M.P.; Poznjakovskiy, V.M.; de la Mora, J.F. Correlations for Vapor Nucleating CriticalEmbryo Parameters. *J. Phys. Chem. Ref. Data* **2003**, *32*, 1387–1410. [CrossRef]

32. Wilson, C.T.R. Condensation of water vapour in the presence of dust-free air and other gases. *Philosophical Trans. R. Soc. Lond.* **1897**, *189*, 265–307. [CrossRef]

33. Gamero-Castano, M.; de la Mora, J.F. A Condensation NucleusCounter (CNC) Sensitive to Singly Charged Sub-Nanometer Particles. *J. Aerosol Sci.* **2000**, *31*, 757–772. [CrossRef]

34. Kim, C.S.; Okuyama, K.; Fernandez de la Mora, J. Performance Evaluation of an Improved Particle Size Magnifier (PSM) for Single Nanoparticle Detection. *Aerosol Sci. Technol.* **2003**, *37*, 791–803. [CrossRef]

35. Iida, K.; Stolzenburg, M.R.; McMurry, P.H. Effect of Working Fluid on Sub-2 nm Particle Detection with a Laminar Flow Ultrafine Condensati on Particle Counter. *Aerosol Sci. Technol.* **2009**, *43*, 81–96. [CrossRef]

36. Vanhanen, J.; Mikkilä, J.; Lehtipalo, K.; Sipilä, M.; Manninen, H.E.; Siivola, E.; Petäjä, T.; Kulmala, M. Particle Size Magnifier for Nano-CN Detection. *Aerosol Sci. Technol.* **2011**, *45*, 533–542. [CrossRef]

37. Wimmer, D.; Lehtipalo, K.; Franchin, A.; Kangasluoma, J.; Kreissl, F.; Kurten, A.; Kupc, A.; Metzger, A.; Mikkila, J.; Petaja, T.; et al. Performance of DiethyleneGlycol-Based Particle Counters in the Sub-3 nm Size Range. *Atmos. Meas. Tech.* **2013**, *6*, 1793–1804. [CrossRef]

38. Hienola, A.I.; Winkler, P.M.; Wagner, P.E.; Vehkamaki, H.; Lauri, A.; Napari, I.; Kulmala, M. Estimation of Line Tension and Contact Angle From Heterogeneous Nucleation Experimental Data. *J. Chem. Phys.* **2007**, *126*, 094705. [CrossRef]

39. Kulmala, M.; Riipinen, I.; Sipila, M.; Manninen, H.E.; Petäjä, T.; Junninen, H.; Maso, M.D.; Mordas, G.; Mirme, A.; Vana, M. Toward Direct Measurement of Atmospheric Nucleation. *Science* **2007**, *318*, 89. [CrossRef]

40. Maisser, A.; Hogan, C.J. Examination of organic vapor adsorption onto alkali metal and halide atomic ions using ion mobility mass spectrometery. *ChemPhysChem* **2017**, *18*, 3039–3046. [CrossRef]

41. Tauber, C.; Chen, X.; Wagner, P.; Winkler, P.; Hoga, C.J.; Maisser, A. Henterogeneous nucleation onto monoatomic ions: support for the Kelvin Thomson theory. *ChemPhysChem* **2018**, *19*, 3144–3149. [CrossRef]

42. Heim, M.; Attoui, M.; Kasper, G. The efficiency of diffu-sional particle collection onto wire grids in the mobility equiv-alent size range of 1.2–8 nm. *J. Aerosol Sci.* **2010**, *41*, 207–222. [CrossRef]

43. Jiang, J.; Attoui, M.; Heim, M.; Brunelli, N.A.; Mc-Murry, P.; Kasper, G.; Flagan, R.C.; Giaspis, K.; Mouret, G. Transfer Functions and Penetrationsof Five Differential Mobility Analyzers for Sub-2 nm Particle Classification. *Aerosol Sci. Technol.* **2011**, *45*, 480–492. [CrossRef]

44. Hering, S.V.; Lewis, G.S.; Spielman, S.R.; Eiguren-Fernandez, A.; Kreisberg, N.M.; Kuang, C.; Attoui, M. Detection near 1-nm with a Laminar-Flow, Water-Based Conden-sation Particle Counter. *Aerosol Sci. Technol.* **2016**, *51*, 354–362. [CrossRef]

45. Kangasluoma, J.; Ahonen, L.; Laurila, T.M.; Cai, R.; Enroth, J.; Mazon, S.B.; Korhonen, F.; Aalto, P.; Kulmala, M.; Attoui, M.; et al. Laboratory verification of a new high flow differential mobility particle sizer and field measurement in Hyytiala. *J. Aerosol Sci.* **2018**, *124*, 1–9. [CrossRef]

46. Cai, R.; Attoui, M.; Jiang, J.; Korhonen, F.; Hao, J.; Petaja, T.; Kangasluoma, J. Characteirzation of a high resolution supercritical differential mobility analyzer at reduced flow rates. *Aerosol Sci. Technol.* **2018**, *52*, 1332–1343. [CrossRef]

47. Fernandez de la Mora, J.; de Juan, L.T.; Eichler, T.; Rosell, J. Differential mobility analysis of molecular ions and nanometerparticles. *Trends Anal.* **1998**, *17*, 328–339. [CrossRef]

48. Hogan, C.; Fernandez de la Mora, J. Ion-Pair Evaporation from Ionic Liquid Clusters. *J. Am. Mass. Spec.* **2010**, *21*, 1382–1386. [CrossRef]

49. Attoui, M.; Fernandez-Garcıa, J.; Cuevas, J.; Vidal, G.; Fernandez de la Mora, J. Charge Evaporation from Nanometer Polystyrene Aerosols. *J. Aerosol Sci.* **2013**, *55*, 149–156. [CrossRef]

50. Higashi, H.; Tokumi, T.; Hogan, C.J.; Suda, H.; Seto, T.; Otani, Y. Simultaneous ion and neutral evaporation in aqueous nanodrops: experiment, theory, and molecular dynamics simulations. *Phys. Chem.* **2015**, *28*, 46–55. [CrossRef]